(5) J. W. Fraser, G. R. Hedwig, H. K. J. Powell, and W. T. Robinson, *Aust. J. Chem.*, **25**, 747 (1972).
(6) S. Bezzi, E. Bua, and G. Schiavinato, *Gazz. Chim. Ital.*, **81**, 856 (1951).
(7) A. Vaciago and L. Zamibonelli, *J. Chem. Soc. A*, 218 (1970).
(8) J. F. Villa and W. E. Hatfield, *J. Chem. Phys.*, **55**, 4758 (1971).
(9) L. E. Godycki and R. E. Rundle, *Acta Crystallogr.*, **6**, 487 (1953).
(10) D. E. Williams, G. Wohlauer, and R. E. Rundle, *J. Am. Chem. Soc.*, **81**, 755 (1959).
(11) B. N. Figgis and J. Lewis, *Mod. Coord. Chem.*, 403 (1960).
(12) Numbers in parentheses here and elsewhere in this paper indicate estimated standard deviations in the least significant digits.
(13) P. Coppens, L. Leiserowitz, and D. Rabinovich, *Acta Crystallogr.*, **18**, 1035 (1965).
(14) D. T. Cromer and J. T. Waber, *Acta Crystallogr.*, **18**, 104 (1945).
(15) R. F. Stewart, E. R. Davidson, and W. T. Simpson, *J. Chem. Phys.*, **42**, 3175 (1965).
(16) D. T. Cromer, *Acta Crystallogr.*, **18**, 17 (1965).
(17) I. B. Bliss and E. O. Schlemper, *Inorg. Chem.*, **14**, 3037 (1975).

Contribution from the Department of Chemistry,
State University of New York at Buffalo, Buffalo, New York 14214

Crystal Structure and Molecular Geometry of the Homogeneous Hydrogenation Catalyst $[(\eta^5\text{-}C_5Me_5)IrCl]_2(\mu\text{-}H)(\mu\text{-}Cl)$ and of Its Precursor $[(\eta^5\text{-}C_5Me_5)IrCl]_2(\mu\text{-}Cl)_2$. A Direct Comparison of $Ir(\mu\text{-}H)(\mu\text{-}Cl)Ir$ and $Ir(\mu\text{-}Cl)_2Ir$ Bridging Systems

MELVYN ROWEN CHURCHILL* and STUART A. JULIS

Received October 1, 1976 AIC60726D

The homogeneous hydrogenation catalyst μ-chloro-μ-hydrido-dichlorobis(pentamethylcyclopentadienyl)diiridium(III), $[(\eta^5\text{-}C_5Me_5)IrCl]_2(\mu\text{-}H)(\mu\text{-}Cl)$, and its synthetic precursor di-μ-chloro-dichlorobis(pentamethylcyclopentadienyl)diiridium(III), $[(\eta^5\text{-}C_5Me_5)IrCl]_2(\mu\text{-}Cl)_2$, have each been studied by means of a single-crystal x-ray structural analysis. Crystal data are as follows. $[(\eta^5\text{-}C_5Me_5)IrCl]_2(\mu\text{-}H)(\mu\text{-}Cl)$: orthorhombic, space group *Pbcn*, $a = 12.493$ (2) Å, $b = 14.454$ (3) Å, $c = 12.860$ (2) Å, $\rho(\text{obsd}) = 2.177$ (5) and $\rho(\text{calcd}) = 2.180$ g cm^{-3} for mol wt 762.2, $V = 2322.1$ (7) Å^3, and $Z = 4$. The molecule has crystallographic C_2 symmetry. $[(\eta^5\text{-}C_5Me_5)IrCl]_2(\mu\text{-}Cl)_2$: monoclinic, space group $P2_1/c$, $a = 8.384$ (1) Å, $b = 9.278$ (1) Å, $c = 15.741$ (2) Å, $\beta = 106.52$ (1)°, $\rho(\text{obsd}) = 2.259$ (7) and $\rho(\text{calcd}) = 2.254$ g cm^{-3} for mol wt 796.7, $V = 1173.8$ (3) Å^3, and $Z = 2$. This species has crystallographic C_i symmetry. Diffraction data for each complex were collected with a Syntex $P2_1$ four-circle diffractometer (Mo Kα radiation; $2\theta(\text{max}) = 40°$) and the structures were solved via the Syntex XTL structure determination system. Final discrepancy indices were $R_F = 4.4\%$ and $R_{wF} = 4.9\%$ for $[(\eta^5\text{-}C_5Me_5)IrCl]_2(\mu\text{-}H)(\mu\text{-}Cl)$ (1089 independent reflections) and $R_F = 3.3\%$ and $R_{wF} = 4.6\%$ for $[(\eta^5\text{-}C_5Me_5)IrCl]_2(\mu\text{-}Cl)_2$ (1095 independent reflections). Each complex is isomorphous and isostructural with its rhodium analogue. Dimensions within the central $Ir(\mu\text{-}H)(\mu\text{-}Cl)Ir'$ bridge of $[(\eta^5\text{-}C_5Me_5)IrCl]_2(\mu\text{-}H)(\mu\text{-}Cl)$ are as follows: Ir···Ir′ = 2.903 (1) Å, Ir–Cl = 2.451 (4) Å, Ir–H = 1.94 (7) Å, Ir–Cl–Ir′ = 72.65 (8)°, Ir–H–Ir′ = 96.9 (25)°, and H–Ir–Cl = 95.2 (17)°. Dimensions within the $Ir(\mu\text{-}Cl)_2Ir'$ bridge of $[(\eta^5\text{-}C_5Me_5)IrCl]_2(\mu\text{-}Cl)_2$ are as follows: Ir···Ir′ = 3.769 (1) Å, Ir–Cl = 2.449 (3) Å, 2.456 (3) Å, Ir–Cl–Ir′ = 100.45 (12)°, and Cl–Ir–Cl′ = 79.55 (12)°. These data are discussed and compared with data previously obtained for the rhodium analogues.

Introduction

We have previously reported the results of x-ray structural analyses of $[(\eta^5\text{-}C_5Me_5)RhCl]_2(\mu\text{-}H)(\mu\text{-}Cl)$[1] and $[(\eta^5\text{-}C_5Me_5)RhCl]_2(\mu\text{-}Cl)_2$.[2] The present structural investigations of the iridium analogues, $[(\eta^5\text{-}C_5Me_5)IrCl]_2(\mu\text{-}H)(\mu\text{-}Cl)$ and $[(\eta^5\text{-}C_5Me_5)IrCl]_2(\mu\text{-}Cl)_2$, were undertaken in order to obtain direct comparisons of $Ir(\mu_2\text{-}H)(\mu_2\text{-}Cl)Ir$ and $Ir(\mu_2\text{-}Cl)_2Ir$ bridges both with each other and with the corresponding $Rh(\mu_2\text{-}H)(\mu_2\text{-}Cl)Rh$ and $Rh(\mu_2\text{-}Cl)_2Rh$ bridges in otherwise identical molecular species. These comparisons are rendered more chemically meaningful (although less crystallographically exciting) by the discovery that $[(\eta^5\text{-}C_5Me_5)IrCl]_2(\mu\text{-}H)(\mu\text{-}Cl)$ is isomorphous with $[(\eta^5\text{-}C_5Me_5)RhCl]_2(\mu\text{-}H)(\mu\text{-}Cl)$ and that $[(\eta^5\text{-}C_5Me_5)IrCl]_2(\mu\text{-}Cl)_2$ is isomorphous with $[(\eta^5\text{-}C_5Me_5)RhCl]_2(\mu\text{-}Cl)_2$.

All four of the above-mentioned species are implicated as powerful catalysts in homogeneous hydrogenation reactions.[3] For both iridium and rhodium, the active catalyst is the μ-chloro-μ-hydrido species. However, this can be generated in situ (under the normal experimental conditions for hydrogenation) from the di-μ-chloro complex by the heterolytic cleavage of dihydrogen (see eq 1).

$$[(\eta^5\text{-}C_5Me_5)MCl]_2(\mu\text{-}Cl)_2 + H_2 \rightarrow [(\eta^5\text{-}C_5Me_5)MCl]_2(\mu\text{-}H)(\mu\text{-}Cl) + HCl \tag{1}$$

Experimental Section

$[(\eta^5\text{-}C_5Me_5)IrCl]_2(\mu\text{-}Cl)_2$ was prepared via the method of Maitlis et al.[4] from the reaction of $IrCl_3 \cdot 3H_2O$ (Ventron) and hexamethyl(Dewar benzene) (Aldrich) in methanol (see eq 2). The product was washed with ether and recrystallized from 1,2-dichloroethane.

2 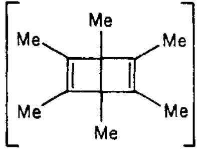

$+ 2IrCl_3 \cdot 3H_2O + 4MeOH$

$$\rightarrow [(\eta^5\text{-}C_5Me_5)IrCl]_2(\mu\text{-}Cl)_2 + 2MeCH(OMe)_2 + 2HCl + 6H_2O \tag{2}$$

Crystals of $[(\eta^5\text{-}C_5Me_5)IrCl]_2(\mu\text{-}H)(\mu\text{-}Cl)$ were supplied by Professor P. M. Maitlis of Sheffield University, Sheffield, England.

Each complex is stable indefinitely in the solid state and does not decompose upon exposure to x-rays.

Collection of X-Ray Diffraction Data

1. $[(\eta^5\text{-}C_5Me_5)IrCl]_2(\mu\text{-}H)(\mu\text{-}Cl)$. The crystal selected for the structural investigation was a red block of maximum dimension 0.13 mm. It was mounted on a thin glass fiber, sealed into a 0.2-mm diameter thin-walled Lindemann glass capillary, and fixed into a eucentric goniometer. The crystal was centered in a random orientation (later found to be with $[\bar{4}45]$ offest by ~0.72° from coincidence with the ϕ axis) on a Syntex $P2_1$ four-circle diffractometer under the control of a NOVA 1200 computer. Axial photographs revealed D_{2h} (*mmm*) Laue symmetry, indicating that the crystal belonged to the orthorhombic crystal class.

Determination of the orientation matrix, measurement of unit cell parameters, checks on peak profile, and data collection were carried out as described previously;[5] details are given in Table I.

Examination of the complete set of intensity data revealed the systematic absences $0kl$ for $k = 2n + 1$, $h0l$ for $l = 2n + 1$, and $hk0$

Table I. Details of Data Collection for $[(\eta^5\text{-}C_5Me_5)IrCl]_2(\mu\text{-}H)(\mu\text{-}Cl)$ and $[(\eta^5\text{-}C_5Me_5)IrCl]_2(\mu\text{-}Cl)_2$

	$(\mu\text{-}H)(\mu\text{-}Cl)$ complex	$(\mu\text{-}Cl)_2$ complex
	(A) Crystal Parameters	
Crystal system	Orthorhombic	Monoclinic
Space group	*Pbcn* [No. 60]	$P2_1/c$ [No. 14]
a, Å	12.493 (2)[a]	8.384 (1)[b]
b, Å	14.454 (3)	9.278 (1)
c, Å	12.860 (2)	15.741 (2)
β, deg		106.52 (1)
V, Å^3	2322.1 (7)	1173.8 (3)
Temp, °C	25.5 (5)	23.0 (5)
Z	4	2
Mol wt	762.2	796.7
ρ(obsd), g cm^{-3}	2.177 (5)[c]	2.259 (7)[c]
ρ(calcd), g cm^{-3}	2.180	2.254
	(B) Collection of Intensity Data[d]	
Radiation	Mo Kα ($\bar{\lambda}$ 0.710 730 Å)	
Monochromator	Highly oriented graphite (equatorial)	
Monochromator angle, deg	12.2	
Takeoff angle, deg	6.9	
Reflections measd	$-h,+k,+l$	$+h,+k,\pm l$
2θ range, deg	6-40	
Scan type	θ(crystal)-2θ(counter)	
Scan speed, deg/min	4	
Scan range	$[2\theta(K\alpha_1) - 1.0]° \rightarrow [2\theta(K\alpha_2) + 1.0]°$	
Background measurement	At beginning and end of the scan	
	Each for one-fourth of the total scan time	Each for one-half of total scan time
Standards	3 every 50 reflections[e]	3 every 47 reflections[f]
Reflections collected	1361 total, 1089 independent (78 check reflections, 194 systematic absences)	1377 total, 1095 independent (87 check reflections, 95 systematic absences)
	(C) Treatment of Intensity Data	
"Ignorance factor"	0.035	0.030
Reflections rejected	None	None
Absorption coeff, cm^{-1}	124.9	117.5

[a] Based on a least-squares fit to the setting angles of the unresolved Mo $K\bar{\alpha}$ peaks of 15 reflections with 2θ = 28-37°. [b] Based on the Mo $K\bar{\alpha}$ peaks of 25 reflections with 2θ = 26-40°. [c] The densities were measured by neutral buoyancy in aqueous zinc iodide. [d] Unless otherwise stated, conditions for data collection on the di-μ-chloro complex parallel those for the μ-chloro-μ-hydrido species. [e] Maximum deviations of intensities from their mean values were 1.6% for 400, 1.7% for 060, and 2.0% for 004. [f] Maximum deviations from the mean were 2.4% for 200, 2.0% for 040, and 2.0% for 004.

for $h + k = 2n + 1$, consistent with the centrosymmetric orthorhombic space group *Pbcn* [$D_{2h}{}^{14}$; No. 60].

Data were corrected for absorption by an empirical method using the program TAPER.[6] Six close-to-axial reflections distributed over the range of 2θ values used in data collection, each being of fairly strong intensity, were measured at 36 points around the diffraction vector (beginning at $\psi = 0°$, ending at $\psi = 350°$, with a ψ increment of 10°). Each reflection defined an absorption curve of intensity vs. ϕ corrected for ω and χ. The curve nearest in 2θ to the Bragg angle of the intensity data reflection was interpolated in ϕ to correct that reflection for absorption. Reflections used for the absorption curves were $\bar{2}33$ (2θ = 14.30°), $\bar{3}34$ (2θ = 18.14°), $\bar{4}45$ (2θ = 23.52°), $\bar{4}56$ (2θ = 27.21°), $\bar{5}67$ (2θ = 32.67°), and $\bar{7}67$ (2θ = 36.57°). The magnitude of the correction was such that values for (maximum intensity)/(minimum intensity) for the six curves were, respectively 1.755, 1.595, 1.565, 1.628, 1.585, and 1.580. The curves were internally consistent—i.e., maximum intensity was observed at the same ϕ value for each reflection, etc.

2. $[(\eta^5\text{-}C_5Me_5)IrCl]_2(\mu\text{-}Cl)_2$. A brown-orange fragment of approximate dimensions 0.20 × 0.28 × 0.33 mm was cut from a larger platelike crystal and was mounted and aligned (with $[12\bar{8}]$ offset by ~1.5° from the ϕ axis) as before. Axial photographs revealed C_{2h} ($2/m$) symmetry, indicating that the crystal belonged to the monoclinic crystal class. Unit cell parameters (determined as before) and details of data collection appear in Table I.

Examination of the data set revealed the systematic absences $h0l$ for $l = 2n + 1$ and $0k0$ for $k = 2n + 1$, consistent only with the centrosymmetric monoclinic space group $P2_1/c$ [$C_{2h}{}^5$; No. 14].

Data were corrected for absorption using TAPER (see above) and absorption curves for the close-to-axial reflections $11\bar{5}$ (2θ = 13.72°; max/min = 1.195), $12\bar{8}$ (22.61°; 1.165), $1,3,\overline{10}$ (29.41°; 1.148), and $2,2,\overline{14}$ (37.89°; 1.156). Again, the curves were internally consistent with similar ϕ-dependent profiles and with maxima and minima observed at essentially the same ϕ values for each reflection.

Solution and Refinement of the Structures

All calculations were performed using the Syntex XTL Structure Determination System (in-house NOVA 1200 computer with 24K, 16-bit word memory; disk unit of 1.2 million 16-bit words; XTL conversational crystallographic program package).[6]

Following correction for absorption (vide supra), all data were corrected for Lorentz and polarization effects, the form of the *Lp* factor being that given in eq 3. (This equation assumes that the graphite

$$Lp = \frac{0.5}{\sin 2\theta}\left[\left(\frac{1 + \cos^2 2\theta_M \cos^2 2\theta}{1 + \cos^2 2\theta_M}\right) + \left(\frac{1 + |\cos 2\theta_M| \cos^2 2\theta}{1 + |\cos 2\theta_M|}\right)\right] \tag{3}$$

monochromator crystal is 50% mosaic and 50% perfect; $2\theta_M$, the monochromator angle, is 12.2° for Mo Kα radiation).

Data were placed on an approximately absolute scale via a Wilson plot.

The analytical scattering factors of Cromer and Mann[7a] for *neutral* atoms were used throughout the analyses; both the real and imaginary components of anomalous dispersion[7b] were used for all nonhydrogen atoms. Discrepancy indices used are defined in eq 4 and 5. The

$$R_F = \left[\frac{\Sigma||F_o| - |F_c||}{\Sigma|F_o|}\right] \times 100\ (\%) \tag{4}$$

$$R_{wF} = \left[\frac{\Sigma w(|F_o| - |F_c|)^2}{\Sigma w|F_o|^2}\right]^{1/2} \times 100\ (\%) \tag{5}$$

weighting scheme used is defined in eq 6, wherein $\sigma_C(F)$ is derived

Table II. Final Positional Parameters (with Esd's) for $[(\eta^5\text{-}C_5Me_5)IrCl]_2(\mu\text{-}H)(\mu\text{-}Cl)^a$

Atom	*x*	*y*	*z*
Ir	0.035 44 (4)	0.191 33 (4)	0.142 49 (4)
Cl(T)	−0.146 77 (29)	0.195 05 (29)	0.084 24 (29)
Cl(B)	0	0.054 73 (35)	$^1/_4$
C(1)	0.094 2 (12)	0.210 8 (10)	−0.014 9 (10)
C(2)	0.104 4 (12)	0.293 1 (9)	0.043 1 (10)
C(3)	0.176 1 (12)	0.271 8 (10)	0.123 0 (11)
C(4)	0.205 7 (11)	0.178 1 (9)	0.120 0 (11)
C(5)	0.155 8 (11)	0.136 7 (10)	0.034 5 (10)
C(6)	0.032 0 (13)	0.200 9 (13)	−0.108 1 (14)
C(7)	0.059 5 (14)	0.381 1 (11)	0.013 5 (12)
C(8)	0.217 7 (13)	0.339 7 (11)	0.202 3 (15)
C(9)	0.282 5 (12)	0.127 9 (12)	0.188 9 (13)
C(10)	0.165 3 (14)	0.039 6 (11)	−0.0045 (11)
H(B)	0	0.280 3 (68)	$^1/_4$
H(6A)	0.052 4	0.226 6	−0.161 0
H(6B)	−0.032 4	0.210 6	−0.113 7
H(6C)	0.020 8	0.123 8	−0.132 9
H(7A)	0.052 3	0.424 3	0.064 0
H(7B)	0.089 8	0.426 6	−0.033 8
H(7C)	−0.018 8	0.371 0	−0.011 2
H(8A)	0.239 8	0.317 0	0.270 2
H(8B)	0.277 8	0.367 7	0.189 7
H(8C)	0.171 0	0.389 7	0.202 2
H(9A)	0.268 7	0.075 8	0.200 7
H(9B)	0.347 7	0.132 9	0.170 5
H(9C)	0.291 8	0.160 1	0.253 5
H(10A)	0.225 1	0.042 0	−0.054 7
H(10B)	0.108 0	0.025 0	−0.047 7
H(10C)	0.182 3	0.001 0	0.041 7

$$w = \{[\sigma_C(F)]^2 + [pF_o]^2\}^{-1} \tag{6}$$

from $\sigma(I)$ based purely on counting statistics. The values used for p (the "ignorance factor") are shown in Table I.

The goodness of fit (GOF) is defined in eq 7. Here, n is the number

$$\text{GOF} = \left[\frac{\Sigma w(|F_o| - |F_c|)^2}{n - v}\right]^{1/2} \tag{7}$$

of observations and v is the number of variables.

1. $[(\eta^5\text{-}C_5Me_5)IrCl]_2(\mu\text{-}H)(\mu\text{-}Cl)$. The structure of $[(\eta^5\text{-}C_5Me_5)IrCl]_2(\mu\text{-}H)(\mu\text{-}Cl)$ was solved from the known coordinates of the isomorphous rhodium species.[1] Full-matrix least-squares refinement of positional parameters for all nonhydrogen atoms, anisotropic thermal parameters for iridium and chlorine atoms, and isotropic thermal parameters for all carbon atoms led to convergence in five cycles with R_F = 5.0%, R_{wF} = 5.8%, and GOF = 1.15.

A difference-Fourier map now showed, clearly, the bridging hydride ligand (at 0, ~0.28, $^1/_4$) but gave equivocal results on the hydrogen atoms of the methyl groups. Refinement was continued, now using anisotropic thermal parameters for all nonhydrogen atoms; hydrogen atoms of the methyl groups were included in fixed positions using coordinates obtained from the study[1] of the isomorphous species $[(\eta^5\text{-}C_5Me_5)RhCl]_2(\mu\text{-}H)(\mu\text{-}Cl)$. Five cycles of refinement led to improvement from R_F = 4.6%, R_{wF} = 5.3%, and GOF = 1.09 (*before* refinement) to the final values R_F = 4.4%, R_{wF} = 4.9%, and GOF = 1.01. During the last cycle of refinement the largest shift was 0.06σ, indicating that convergence had been achieved. The largest peaks on a final difference-Fourier synthesis were of height 0.67 e Å^{-3} (at 0.50, 0.40, 0.15 and 0.00, 0.12, 0.25). The structure is thus both correct and complete.

The function $\Sigma w(|F_o| - |F_c|^2)$ showed no appreciable variation as a function of $|F_o|$, $(\sin\theta)/\lambda$, identity or parity of Miller indices, or sequence number. The weighting scheme is thus satisfactory. There is no evidence of secondary extinction. Final positional and thermal parameters are collected in Tables II and III.

2. $[(\eta^5\text{-}C_5Me_5)IrCl]_2(\mu\text{-}Cl)_2$. This structure was solved by direct methods (using MULTAN) and found to be isostructural with the rhodium analogue.[2] Six cycles of full-matrix least-squares refinement of positional and isotropic thermal parameters for all nonhydrogen atoms led to R_F = 4.3%, R_{wF} = 6.3%, and GOF = 1.34. Attempts to locate the hydrogen atoms from difference-Fourier maps were uniformly unsuccessful. (This is not surprising considering (i) the presence of an iridium and two chlorine atoms in the asymmetric unit and (ii) the magnitude of the librational motion of the pentamethylcyclopentadienyl ligand.) Refinement was continued, now using anisotropic thermal parameters for all nonhydrogen atoms. Six cycles of full-matrix least-squares refinement led to final convergence [Δ_{max} = 0.01σ] with R_F = 3.3%, R_{wF} = 4.6%, and GOF = 1.00. The largest peak on a final difference-Fourier synthesis was of height 0.83 e Å^{-3} at 0.24, 0.04, 0.04 (i.e., close to the position of the iridium atom). The correctness of the structure is thus confirmed. The function $\Sigma w(|F_o| - |F_c|)^2$ was, again, essentially independent of $|F_o|$, $(\sin\theta)/\lambda$, parity or identity of Miller indices, or sequence number. The weighting scheme is thus satisfactory.

Final positional and thermal parameters are given in Tables IV and V.

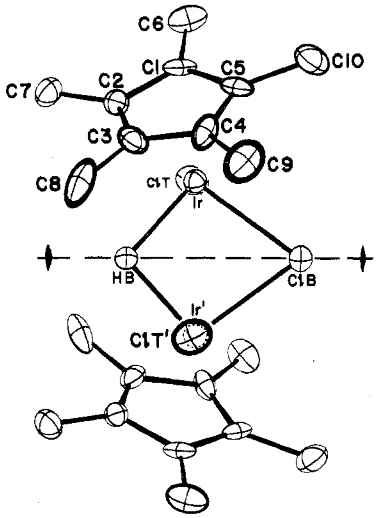

Figure 1. The $[(\eta^5\text{-}C_5Me_5)IrCl]_2(\mu\text{-}H)(\mu\text{-}Cl)$ molecule, projected onto its Ir(μ-H)(μ-Cl)Ir′ plane. The crystallographic C_2 axis is shown [ORTEP diagram; 30% probability thermal ellipsoids].

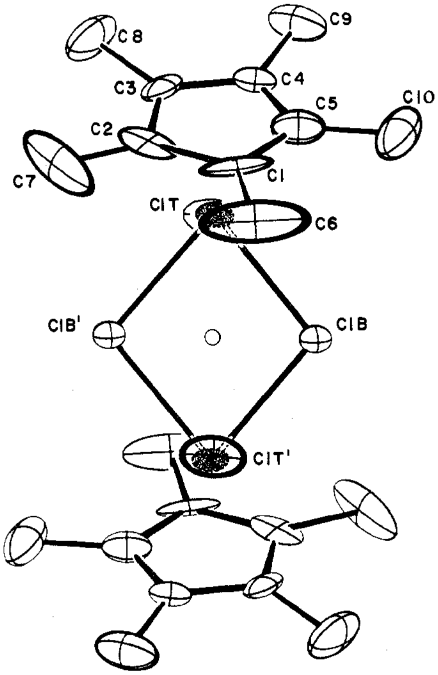

Figure 2. The $[(\eta^5\text{-}C_5Me_5)IrCl]_2(\mu\text{-}Cl)_2$ molecule, projected onto its Ir(μ-Cl)Ir′ plane. The center of symmetry is designated by a hollow circle. Iridium atoms are stippled [ORTEP diagram; 30% ellipsoids].

Discussion

Interatomic distances and angles for the two species are collected in Tables VI and VII. The $[(\eta^5\text{-}C_5Me_5)IrCl]_2(\mu\text{-}H)(\mu\text{-}Cl)$ molecule is shown, projected onto its Ir(μ-H)(μ-

Table III. Anisotropic Thermal Parameters[a,b] (with Esd's) for $[(\eta^5\text{-}C_5Me_5)IrCl]_2(\mu\text{-}H)(\mu\text{-}Cl)$

Atom	B_{11}	B_{22}	B_{33}	B_{12}	B_{13}	B_{23}
Ir	2.58 (3)	2.47 (3)	2.64 (3)	0.11 (2)	0.04 (2)	0.11 (2)
Cl(T)	3.09 (17)	5.20 (22)	3.75 (18)	0.43 (17)	−0.65 (15)	−0.48 (16)
Cl(B)	3.76 (25)	2.55 (25)	3.39 (23)	0	0.27 (20)	0
C(1)	3.0 (7)	5.4 (9)	1.5 (6)	0.6 (7)	0.7 (6)	0.4 (6)
C(2)	3.6 (7)	2.8 (7)	2.7 (6)	0.8 (6)	−0.1 (6)	0.2 (6)
C(3)	3.2 (7)	3.2 (7)	3.3 (6)	0.1 (6)	0.9 (6)	−0.9 (6)
C(4)	2.1 (6)	2.5 (7)	4.7 (7)	0.6 (6)	0.2 (6)	1.3 (6)
C(5)	3.0 (7)	4.4 (8)	1.8 (6)	−0.2 (6)	0.9 (5)	−0.7 (6)
C(6)	5.2 (11)	7.3 (13)	4.3 (9)	−0.4 (9)	1.5 (7)	0.9 (8)
C(7)	6.1 (10)	3.5 (8)	3.5 (7)	−0.3 (7)	−0.7 (7)	0.8 (6)
C(8)	4.3 (9)	3.2 (9)	8.3 (11)	0.5 (7)	0.3 (8)	2.7 (8)
C(9)	3.0 (7)	5.0 (9)	5.9 (9)	0.7 (7)	0.1 (7)	1.5 (8)
C(10)	5.8 (9)	4.9 (10)	3.8 (9)	1.9 (8)	0.1 (7)	−0.8 (8)

[a] The anisotropic thermal parameters (units Å^2) enter the equation for the calculated structure factor in the form $\exp[-0.25(B_{11}h^2a^{*2} + B_{22}k^2b^{*2} + B_{33}l^2c^{*2} + 2B_{12}hka^*b^* + 2B_{13}hla^*c^* + 2B_{23}klb^*c^*)]$. [b] Isotropic thermal parameters: H(B), B = 2.4 (19) Å^2; all other H's, B = 7.0 Å.

Table IV. Final Positional Parameters (with Esd's) for $[(\eta^5\text{-}C_5Me_5)IrCl]_2(\mu\text{-}Cl)_2$

Atom	x	y	z
Ir	0.189 54 (5)	0.037 34 (5)	0.095 68 (3)
Cl(B)	0.107 50 (37)	0.014 91 (36)	0.066 45 (20)
Cl(T)	0.241 80 (47)	−0.215 81 (37)	0.108 34 (24)
C(1)	0.236 8 (20)	0.262 0 (13)	0.108 3 (8)
C(2)	0.188 3 (16)	0.208 7 (16)	0.184 4 (11)
C(3)	0.315 6 (17)	0.107 3 (15)	0.225 8 (7)
C(4)	0.433 7 (14)	0.101 0 (14)	0.175 0 (8)
C(5)	0.384 9 (17)	0.191 0 (15)	0.105 1 (9)
C(6)	0.141 1 (27)	0.377 4 (17)	0.045 6 (14)
C(7)	0.047 1 (21)	0.248 5 (27)	0.221 0 (17)
C(8)	0.336 4 (30)	0.021 9 (21)	0.313 5 (11)
C(9)	0.592 3 (21)	0.008 3 (19)	0.198 3 (13)
C(10)	0.479 8 (23)	0.216 2 (21)	0.035 9 (9)

Cl)Ir′ plane, in Figure 1. A projection of the $[(\eta^5\text{-}C_5Me_5)IrCl]_2(\mu\text{-}Cl)_2$ molecule onto its $Ir(\mu\text{-}Cl)_2Ir'$ bridge plane is presented in Figure 2.

The $[(\eta^5\text{-}C_5Me_5)IrCl]_2(\mu\text{-}H)(\mu\text{-}Cl)$ molecule has precise C_2 symmetry with the two crystallographically related $[(\eta^5\text{-}C_5Me_5)IrCl]$ residues being bridged by a chloride [Cl(B)] and a hydride ligand [H(B)], each of which lies on the twofold axis (at $x = 0$ and $z = {}^1/_2$).

The $[(\eta^5\text{-}C_5Me_5)IrCl]_2(\mu\text{-}Cl)_2$ molecule has precise C_i symmetry, its two $[(\eta^5\text{-}C_5Me_5)IrCl]$ fragments being mutually coupled via two bridging chloride ligands, Cl(B) and Cl(B)′.

The diamagnetic molecules are best described as iridium(III) complexes in which the coordination geometry about iridium resembles three-legged piano stools. Projections of portions of the two molecules onto their pentatomic carbocyclic rings are shown in Figures 3 and 4. Angles between the monatomic ligands are all close to the ideal octahedral value [the $\eta^5\text{-}C_5Me_5^-$ ligand being conventionally designated as a quasi-tridentate, six-electron donor]; within the $[(\eta^5\text{-}C_5Me_5)IrCl]_2(\mu\text{-}H)(\mu\text{-}Cl)$ molecule these angles are Cl(T)–Ir–Cl(B) = 91.31 (12)°, Cl(T)–Ir–H(B) = 89.5 (17)°, and Cl(B)–Ir–H(B) = 95.2 (17)°; corresponding angles within the $[(\eta^5\text{-}C_5Me_5)IrCl]_2(\mu\text{-}Cl)_2$ molecule are Cl(T)–Ir–Cl(B) = 89.65 (12)°, Cl(T)–Ir–Cl(B)′ = 88.49 (12)°, and Cl(B)–Ir–Cl(B)′ = 79.55 (12)°.

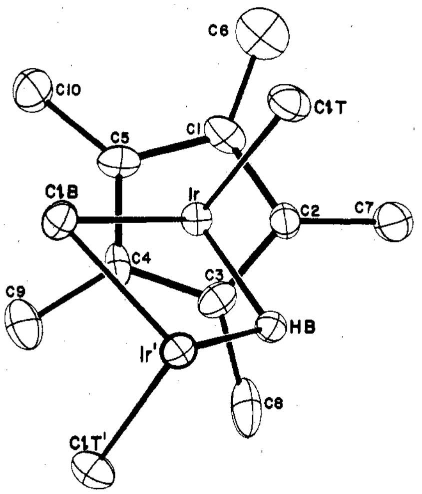

Figure 3. A portion of the $[(\eta^5\text{-}C_5Me_5)IrCl]_2(\mu\text{-}H)(\mu\text{-}Cl)$ molecule projected onto the carbocyclic ring, showing the relative orientations of the $\eta^5\text{-}C_5Me_5$ ring and the three monatomic ligands about the $Ir\text{–}C_5Me_5$ axis.

In each complex the iridium–(terminal chloride) bond length is, as expected, slightly, but significantly, shorter than the iridium–(bridging chloride) distance(s). Appropriate values are Ir–Cl(T) = 2.397 (4) Å and Ir–Cl(B) = 2.451 (4) Å [difference 0.054 (6) Å] for the μ-chloro-μ-hydrido species and Ir–Cl(T) = 2.387 (4) Å and Ir–Cl(B)(av) = 2.453 ± 0.005

Table V. Anisotropic Thermal Parameters (with Esd's) for $[(\eta^5\text{-}C_5Me_5)IrCl]_2(\mu\text{-}Cl)_2$[a]

Atom	B_{11}	B_{22}	B_{33}	B_{12}	B_{13}	B_{23}
Ir	2.49 (3)	2.22 (4)	2.59 (3)	0.07 (1)	−0.38 (2)	−0.35 (1)
Cl(B)	2.93 (15)	4.97 (16)	2.89 (14)	−0.83 (12)	0.51 (12)	−0.85 (12)
Cl(T)	5.47 (17)	2.44 (16)	6.89 (19)	0.42 (15)	−1.00 (15)	−0.17 (14)
C(1)	6.9 (9)	0.8 (6)	3.9 (7)	−0.2 (6)	−4.1 (7)	0.2 (5)
C(2)	3.3 (7)	3.7 (7)	8.4 (10)	−1.8 (6)	−0.4 (7)	−4.3 (8)
C(3)	5.4 (8)	4.9 (8)	1.9 (5)	−1.7 (7)	−0.2 (5)	−1.2 (5)
C(4)	3.0 (6)	3.3 (6)	4.0 (6)	−0.6 (5)	−0.7 (5)	−0.6 (6)
C(5)	4.9 (7)	2.9 (6)	5.2 (7)	−0.6 (6)	−0.6 (6)	−0.9 (6)
C(6)	13.4 (15)	2.2 (7)	12.4 (13)	1.3 (9)	−7.6 (12)	−0.7 (9)
C(7)	4.9 (8)	17.3 (20)	22.9 (21)	−2.8 (11)	6.8 (12)	−16.9 (19)
C(8)	12.4 (16)	10.7 (13)	3.2 (7)	−4.4 (11)	1.2 (9)	1.5 (8)
C(9)	4.2 (8)	6.7 (8)	8.9 (12)	1.0 (7)	−0.9 (8)	−2.0 (8)
C(10)	12.0 (13)	9.5 (12)	4.9 (7)	−6.2 (11)	3.7 (8)	−2.4 (8)

[a] See footnote *a* to Table III.

Table VI. Intramolecular Distances (Å) with Esd's

	(μ-H)(μ-Cl) complex	(μ-Cl)$_2$ complex
(A) Distances from the Iridium Atom		
Ir···Ir′	2.903 (1)	3.769 (1)
Ir-Cl(T)	2.397 (4)	2.387 (4)
Ir-Cl(B)	2.451 (4)	2.456 (3)
Ir-Cl(B)′		2.449 (3)
Ir-H(B)	1.939 (65)	
Ir-C(1)	2.172 (13)	2.121 (12)
Ir-C(2)	2.131 (13)	2.118 (16)
Ir-C(3)	2.122 (15)	2.121 (11)
Ir-C(4)	2.155 (13)	2.155 (12)
Ir-C(5)	2.194 (13)	2.144 (14)
Av Ir-C	2.155	2.132
(B) Carbon-Carbon Distances		
C(1)-C(2)	1.410 (19)	1.457 (21)
C(2)-C(3)	1.398 (20)	1.432 (20)
C(3)-C(4)	1.404 (20)	1.439 (18)
C(4)-C(5)	1.398 (19)	1.349 (18)
C(5)-C(1)	1.464 (20)	1.419 (22)
Av C(sp^2)-C(sp^2)	1.415	1.419
C(1)-C(6)	1.435 (22)	1.520 (23)
C(2)-C(7)	1.441 (21)	1.502 (25)
C(3)-C(8)	1.508 (23)	1.558 (21)
C(4)-C(9)	1.494 (21)	1.538 (22)
C(5)-C(10)	1.496 (22)	1.538 (22)
Av C-Me	1.475	1.531

Table VII. Interatomic Angles (deg) with Esd's

	(μ-H)(μ-Cl) complex	(μ-Cl)$_2$ complex
(A) Angles within Ir(μ-X)(μ-Cl)Ir Bridges		
Ir-Cl(B)-Ir′	72.65 (8)	100.45 (12)
Ir-Cl(B)′-Ir′		100.45 (12)
Ir-H(B)-Ir′	96.9 (25)	
Cl(B)-Ir-Cl(B)′		79.55 (12)
Cl(B)-Ir′-Cl(B)′		79.55 (12)
Cl(B)-Ir-H(B)	95.2 (17)	
Cl(B)-Ir′-H(B)	95.2 (17)	
Ir′···Ir-Cl(B)	53.67 (7)	39.71 (8)
Ir′···Ir-Cl(B)′		39.84 (8)
Ir′···Ir-H(B)	41.5 (17)	
(B) Angles Involving Cl(T)		
Cl(T)-Ir-Cl(B)	91.31 (12)	89.65 (12)
Cl(T)-Ir-Cl(B)′		88.49 (12)
Cl(T)-Ir-H(B)	89.5 (17)	
(C) Internal Angles of the (η^5-C$_5$Me$_5$) Ligand		
C(5)-C(1)-C(2)	109.9 (12)	108.8 (12)
C(1)-C(2)-C(3)	105.1 (12)	104.5 (12)
C(2)-C(3)-C(4)	111.2 (12)	108.4 (12)
C(3)-C(4)-C(5)	108.5 (12)	109.3 (12)
C(4)-C(5)-C(1)	105.2 (12)	108.9 (12)
Av	108.0	108.0
(D) External Angles of the (η^5-C$_5$Me$_5$) Ligand		
C(5)-C(1)-C(6)	125.1 (13)	127.6 (14)
C(2)-C(1)-C(6)	125.0 (14)	123.6 (14)
C(1)-C(2)-C(7)	124.8 (13)	131.8 (15)
C(3)-C(2)-C(7)	129.7 (13)	123.6 (15)
C(2)-C(3)-C(8)	125.1 (13)	128.2 (13)
C(4)-C(3)-C(8)	123.8 (13)	123.4 (13)
C(3)-C(4)-C(9)	128.4 (13)	125.1 (12)
C(5)-C(4)-C(9)	123.0 (13)	125.6 (13)
C(4)-C(5)-C(10)	129.0 (13)	125.1 (13)
C(1)-C(5)-C(10)	125.7 (12)	126.0 (13)
Av	126.0	126.0

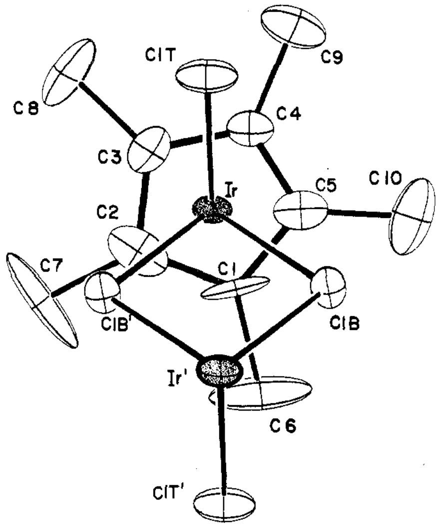

Figure 4. A portion of the [(η^5-C$_5$Me$_5$)IrCl]$_2$(μ-Cl)$_2$ molecule, projected onto the carbocyclic ring C$_5$Me$_5$ ring. (Iridium atoms are stippled for clarity.)

Table VIII. Least-squares Planes and Deviations of Atoms Therefrom[a]

Atom	Dev, Å	Atom	Dev, Å
(A) [(η^5-C$_5$Me$_5$)IrCl]$_2$(μ-H)(μ-Cl) Molecule[b]			
Plane I: $0.7819X + 0.2449Y - 0.5733Z - 1.7592 = 0$[d]			
C(1)*	0.017 (14)	C(6)	0.061 (17)
C(2)*	−0.019 (14)	C(7)	0.071 (17)
C(3)*	0.016 (14)	C(8)	0.079 (17)
C(4)*	−0.004 (13)	C(9)	0.061 (16)
C(5)*	−0.008 (13)	C(10)	0.029 (16)
Ir	−1.7864 (5)		
Plane II: $0.7818X + 0.2370Y - 0.5767Z - 1.7916 = 0$			
C(6)*	0.011 (17)	C(9)*	0.006 (16)
C(7)*	−0.005 (17)	C(10)*	−0.008 (16)
C(8)*	−0.001 (17)		
Plane III: $-0.9523X - 0.3050Z + 0.9806 = 0$[d]			
Ir*	0.000	Cl(B)*	0.000
Ir′*	0.000	H(B)*	0.000
(B) [(η^5-C$_5$Me$_5$)IrCl]$_2$(μ-Cl)$_2$ Molecule[c]			
Plane I: $-0.3912X - 0.7320Y - 0.5578Z + 3.2691 = 0$[e]			
C(1)*	−0.009 (13)	C(6)	−0.061 (19)
C(2)*	0.005 (16)	C(7)	−0.045 (25)
C(3)*	0.000 (13)	C(8)	−0.072 (20)
C(4)*	−0.006 (13)	C(9)	−0.052 (18)
C(5)*	0.009 (14)	C(10)	−0.012 (18)
Ir	1.7563 (4)		
Plane II: $-0.3954X - 0.7338Y - 0.5525Z + 3.3158 = 0$			
C(6)*	−0.021 (19)	C(9)*	−0.007 (18)
C(7)*	0.017 (25)	C(10)*	0.017 (18)
C(8)*	−0.007 (20)		
Plane III: $-0.1850X + 0.9790Y - 0.0861Z = 0$[e]			
Ir*	0.000	Cl(B)*	0.000
Ir′*	0.000	Cl(B)′*	0.000

[a] Atoms marked with an asterisk were given unit weight; all other atoms were assigned zero weight. [b] Cartesian coordinates [X, Y, Z] = [ax, by, cz]. [c] Cartesian coordinates [X, Y, Z] = [$ax + cz \cos \beta$, by, $cz \sin \beta$]. [d] Dihedral angle plane 1-plane III = 124.7°. [e] Dihedral angle plane I-plane III = 126.6°.

Å[8] [difference 0.066 (6) Å] for the di-μ-chloro species.

Within the [(η^5-C$_5$Me$_5$)IrCl]$_2$(μ-H)(μ-Cl) molecule, individual iridium–carbon distances involving the carbocyclic ring show significant variations, possibly due to the carbon atoms experiencing differing intramolecular repulsions; thus, the shortest distance, Ir–C(3) = 2.122 (15) Å, involves the carbon atom that lies above H(B), whereas the longer distances, Ir–C(5) = 2.194 (13) Å, Ir–C(1) = 2.172 (13) Å, and Ir–C(4) = 2.155 (13) Å, involve carbon atoms which interact with Cl(T) or Cl(B). The average Ir–C distance is 2.155 Å and the carbocyclic system is, not withstanding the above comments, planar within the limits of experimental error (the

Table IX. Comparative Geometry of $M(\mu\text{-}X)(\mu\text{-}Cl)M$ Bridges in $[(\eta^5\text{-}C_5Me_5)MCl]_2(\mu\text{-}X)(\mu\text{-}Cl)$ Molecules (M = Ir, Rh; X = H, Cl)

	$Ir(\mu\text{-}H)(\mu\text{-}Cl)Ir$ complex	$Rh(\mu\text{-}H)(\mu\text{-}Cl)Rh$ complex[a]	$Ir(\mu\text{-}Cl)_2Ir$ complex	$Rh(\mu\text{-}Cl_2)Rh$ complex[b]
		(A) Distances, Å		
M···M	2.903 (1)	2.906 (1)	3.769 (1)	3.719 (1)
M-Cl(B)	2.451 (4)	2.437 (2)	2.453 (5)[c]	2.459 (9)[c]
M-Cl(T)	2.397 (4)	2.393 (2)	2.387 (4)	2.397 (1)
M-H(B)	1.939 (65)	1.849 (47)		
M-C, av	2.155	2.151	2.132	2.128
		(B) Angles, deg		
M-Cl(B)-M′	72.65 (8)	73.20 (6)	100.45 (12)	98.29 (3)
M-H(B)-M′	96.9 (25)	103.6 (37)		
Cl(B)-M-H(B)	95.2 (17)	91.6 (10)		
Cl(B)-M-Cl(B)′			79.55 (12)	81.71 (3)

[a] See ref 1. [b] See ref 2. [c] Average of two values.

rms deviation from planarity is 0.016 Å—see plane I of Table VIIIA). The iridium atom lies 1.7864 (5) Å below the plane of the five-membered ring. The five methyl substituents are not coplanar with their carbocyclic ring, but each is bent out of the plane in a direction away from the iridium atom. [Individual displacements are 0.061 (17) Å for C(6), 0.071 (17) Å for C(7), 0.079 (17) Å for C(8), 0.061 (16) Å for C(9), and 0.029 (16) Å for C(10); the average such displacement is 0.060 Å.]

Within the $[(\eta^5\text{-}C_5Me_5)IrCl]_2(\mu\text{-}Cl)_2$ molecule, there are no marked variations in the Ir–C bond lengths. These distances range from Ir–C(2) = 2.118 (16) Å to Ir–C(4) = 2.155 (12) Å, the mean value being 2.132 ± 0.017 Å.[8] The pentatomic ring is planar (rms deviation 0.007 Å–see plane I, Table VIIIB), the iridium atom lies 1.7563 (4) Å below this plane, and methyl substituents again bend from this plane in a direction away from the iridium atom by amounts varying from 0.012 (18) Å [for C(10)] to 0.072 (20) Å [for C(8)] and averaging 0.048 Å.

Carbon–carbon distances and C–C–C angles within each species have the expected values—see Tables VI and VII.

Table IX compares the geometry of the species $[(\eta^5\text{-}C_5Me_5)IrCl]_2(\mu\text{-}H)(\mu\text{-}Cl)$ and $[(\eta^5\text{-}C_5Me_5)IrCl]_2(\mu\text{-}Cl)_2$ both with each other and with their rhodium analogues.

The dimensions within each pair of iridium and rhodium analogues are remarkably similar. However, that we do, indeed, have complexes with different heavy-metal atoms is shown unambiguously by (i) satisfactory agreement between observed and calculated density for each complex, (ii) the satisfactory behavior of the anisotropic thermal parameters of the metal atoms under least-squares refinement, (iii) "clean" final difference Fourier syntheses, (iv) detailed differences in the observed structure factor amplitudes of the isomorphous species, and (v) minor, but statistically significant, differences in unit cell dimensions and atomic coordinates.

We note here that the oft-quoted tabulation of ionic radii by Shannon and Prewitt[9] suggested *ionic* radii of 0.87 Å for $^{VI}Ir^{3+}$ and 0.805 Å for $^{VI}Rh^{3+}$ (based upon $r(^{VI}F^-) = 1.19$ Å) or 0.73 Å for $^{VI}Ir^{3+}$ and 0.665 Å for $^{VI}Rh^{3+}$ (based upon $r(^{VI}O^{2-}) = 1.40$ Å). In either case, the *ionic* radius of Ir^{3+} was estimated to be 0.065 Å greater than the corresponding value for Rh^{3+}. However, an extremely recent update of this tabulation by Shannon[10] gives modified "crystal radii" of 0.82 Å for $^{VI}Ir^{3+}$ and 0.805 Å for $^{VI}Rh^{3+}$ and "effective atomic radii" of 0.68 and 0.665 Å (respectively) for these two species, indicating a difference of only 0.015 Å. Similarly, the average metal–metal bond lengths in the organometallic species $Rh_4(CO)_{12}$[11] and $Ir_4(CO)_{12-n}(PPh_3)_n$ (n = 2, 3)[12] are indistinguishable at 2.73 Å.

Our current results suggest that the *covalent* radii for Ir^{III} and Rh^{III} in quasi-octahedral ("three-legged piano stool") coordination are indistinguishable. [Applying Pauling's covalent radius of 0.99 Å for chlorine to all four metal–(terminal chloride) bonds in Table IX, one arrives at covalent radii of 1.402 ± 0.007 Å for Ir^{III} and 1.405 ± 0.003 Å for Rh^{III}.] These results indicate that dramatic effects from the lanthanide contraction can be felt further to the right-hand side of the periodic table than had previously been realized (i.e., are not restricted just to derivatives of hafnium, tantalum, tungsten, and rhenium).

The results in Table IX show that the geometry of the μ-chloro-μ-hydrido species varies from that of the di-μ-chloro species in three important (and interelated) respects.

(1) The iridium–iridium distance of 2.903 (1) Å in $[(\eta^5\text{-}C_5Me_5)IrCl]_2(\mu\text{-}H)(\mu\text{-}Cl)$ and the rhodium–rhodium distance of 2.906 (1) Å in $[(\eta^5\text{-}C_5Me_5)Rh]_2(\mu\text{-}H)(\mu\text{-}Cl]$ are each only about 0.10 Å longer than expected for normal metal–metal single bonds. [Predicted values are 2.804 ± 0.014 Å for Ir^{III}–Ir^{III} and 2.810 ± 0.006 Å for Rh^{III}–Rh^{III}, based on the covalent radii calculated above.] A difference of ~0.10 Å between "bent" $M(\mu_2\text{-}H)M$ bonds and direct M–M bonds appears to be typical, based on our previous experience with $Os_3(CO)_{11}(\mu_2\text{-}H)(H)$ vs. $Os_3(CO)_{12}$[13] and with a variety of triangulated polynuclear rhenium carbonyl hydrides.[14-16] In contrast to this, intramolecular metal···metal distances in the di-μ-chloro species are each more than 0.9 Å longer than the normal single-bond distance (individual values being 3.769 (1) Å for Ir···Ir and 3.719 (1) Å for Rh···Rh), clearly indicating that metal–metal bonding is absent in these molecules.

Note that the above comparisons also suggest that the bridging chloride ligand plays a dormant role in determining the metal–metal distance in the hydrido-bridged species $[(\eta^5\text{-}C_5Me_5)IrCl]_2(\mu\text{-}H)(\mu\text{-}Cl)$ and $[(\eta^5\text{-}C_5Me_5)RhCl]_2(\mu\text{-}H)(\mu\text{-}Cl)$.

(2) Within the μ-chloro-μ-hydrido species, the Ir–Cl(B)–Ir and Rh–Cl(B)–Rh angles are markedly acute—individual values are 72.65 (8) and 73.20 (6)°, respectively. These angles are grossly different from the metal–(bridging chloride)–metal angles in the di-μ-chloro species, where we have Ir–Cl(B)–Ir = 100.45 (12)° and Rh–Cl(B)–Rh = 98.29 (3)°.

These results strongly suggest that the $Ir(\mu\text{-}H)Ir$ and $Rh(\mu\text{-}H)Rh$ systems are held together by closed two-electron three-center bonds in which there is substantial direct metal bonding; the $M(\mu\text{-}H)(\mu\text{-}Cl)M$ cores of these molecules may thus be depicted as in I.

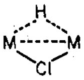

I

(3) The Cl(B)–Ir–H(B) angle in $[(\eta^5\text{-}C_5Me_5)IrCl]_2(\mu\text{-}H)(\mu\text{-}Cl)$ is 95.2 (17)° and the Cl(B)–Rh–H(B) angle in $[(\eta^5\text{-}C_5Me_5)RhCl]_2(\mu\text{-}H)(\mu\text{-}Cl)$ is 91.6 (10)°. Within the di-μ-chloro species there appear to be metal···metal repulsions,

the Cl(B)–Ir–Cl(B)′ and Cl(B)–Rh–Cl(B)′ angles being acute, with values of 79.55 (12) and 81.71 (3)°, respectively.

A final point of possible relevance is the observation that the M⋯M distances in the $[(\eta^5\text{-}C_5Me_5)MCl]_2(\mu\text{-}Cl)_2$ species vary significantly, with values of 3.769 (1) Å for Ir⋯Ir and 3.719 (1) Å for Rh⋯Rh; in contrast to this, there is no significant difference between the Ir–Ir and Rh–Rh distances within the $[(\eta^5\text{-}C_5Me_5)MCl]_2(\mu\text{-}H)(\mu\text{-}Cl)$ species. This observation might be applicable as further evidence for direct metal–metal bonding in the μ-chloro-μ-hydrido species. However, further data are clearly required. We are currently attempting to synthesize μ-bromo-μ-hydrido and di-μ-bromo analogues in the expectation of clarifying these problems.

Acknowledgment. This work was supported by the National Science Foundation through Grant No. CHE76-05564.

Registry No. $[(\eta^5\text{-}C_5Me_5)IrCl]_2(\mu\text{-}Cl)_2$, 12354-84-6; $[(\eta^5\text{-}C_5Me_5)IrCl]_2(\mu\text{-}H)(\mu\text{-}Cl)$, 62078-94-8.

Supplementary Material Available: Listings of structure factor amplitudes (41 pages). Ordering information is given on any current masthead page.

References and Notes

(1) M. R. Churchill and S. W. -Y. Ni, *J. Am. Chem. Soc.*, **95**, 2150 (1973).

(2) M. R. Churchill, S. A. Julis, and F. J. Rotella, *Inorg. Chem.*, **16**, 1137 (1977).

(3) C. White, D. S. Gill, J. W. Kang, H. B. Lee, and P. M. Maitlis, *J. Chem. Soc., Chem. Commun.*, 734 (1971); C. White, A. J. Oliver, and P. M. Maitlis, *J. Chem. Soc., Dalton Trans.*, 1901 (1973), and references contained therein.

(4) J. W. Kang, K. Moseley, and P. M. Maitlis, *J. Am. Chem. Soc.*, **91**, 5970 (1969).

(5) M. R. Churchill, R. A. Lashewycz, and F. J. Rotella, *Inorg. Chem.*, **16**, 265 (1977).

(6) "Syntex XTL Operations Manual", 2nd ed, Syntex Analytical Instruments, Cupertino, Calif., 1976.

(7) "International Tables for X-Ray Crystallography", Vol. IV, Kynoch Press, Birmingham, England, 1974: (a) pp 99–101; (b) pp 149–150.

(8) Esd's on average values are calculated from the "scatter formula", viz.

$$\sigma(\text{av}) = \left[\sum_{i=1}^{i=N} (d_i - \bar{d})^2/(N-1)\right]^{1/2}$$

Here $\bar{d}$ is the average of N equivalent measurement and d_i is the ith such measurement.

(9) R. D. Shannon and C. T. Prewitt, *Acta Crystallogr., Sect. B*, **25**, 925 (1969).

(10) R. D. Shannon, *Acta Crystallogr., Sect. A*, **32**, 751 (1976).

(11) C. H. Wei, G. R. Wilkes, and L. F. Dahl, *J. Am. Chem. Soc.*, **89**, 4792 (1967).

(12) V. Albano, P. Bellon, and V. Scatturin, *Chem. Commun.*, 730 (1967).

(13) M. R. Churchill and B. G. DeBoer, *Inorg. Chem.*, **16**, 878 (1977).

(14) $[H_2Re_3(CO)_{12}^-]$: M. R. Churchill, P. H. Bird, H. D. Kaesz, R. Bau, and B. Fontal, *J. Am. Chem. Soc.*, **90**, 7135 (1968).

(15) $[HRe_3(CO)_{12}^{2-}]$: S. W. Kirtley, H. D. Kaesz, M. R. Churchill, and C. Knobler, in preparation; see also H. D. Kaesz, *Chem. Br.*, **9**, 344 (1973).

(16) $[H_6Re_4(CO)_{12}^{2-}]$: H. D. Kaesz, B. Fontal, R. Bau, S. W. Kirtley, and M. R. Churchill, *J. Am. Chem. Soc.*, **91**, 1021 (1969).

Contribution from the Department of Chemistry, University of North Carolina, Chapel Hill, North Carolina 27514, and the Department of Inorganic Chemistry, University of Sydney, Sydney 2006, Australia

Tridentate Coordination by the L-Cysteine Dianion. Crystal and Molecular Structure of Sodium Bis(L-cysteinato)chromate(III) Dihydrate

PATRICE de MEESTER,[1a] DEREK J. HODGSON,*[1a] HANS C. FREEMAN,*[1b] and CHRISTOPHER J. MOORE[1b]

Received August 9, 1976 AIC605823

The crystal and molecular structure of the title complex, $Na[Cr(\text{L-cys})_2]\cdot 2H_2O$, $C_6H_{14}CrN_2NaO_6S_2$, has been determined from x-ray three-dimensional data. The complex crystallizes in the space group $P3_121$ of the trigonal system with a cell of dimensions $a = 10.644$ (2) and $c = 9.809$ (3) Å. There are three formula units per cell. Full-matrix least-squares refinement using 1221 independent reflections has reached $R = 0.022$. The structure contains $[Cr(\text{L-cys})_2]^-$ anions, sodium cations, and two water molecules of solvation. The Cr and Na atoms as well as the oxygen atoms of the water molecules lie in special positions on diad axes. The complex anion has its central Cr atom in a slightly distorted octahedral coordination with two Cr–S, two Cr–O, and two Cr–N bonds respectively at distances 2.416 (1), 1.981 (1), and 2.062 (2) Å. Cis angles at the Cr atom range from 82.83 (6) to 94.33 (5)°. The two carboxylate oxygens and the two amino nitrogen atoms are mutually cis, while the two sulfur atoms are trans. The sodium cation has a more severely distorted octahedral geometry with its six coordination sites occupied by two pairs of water molecules and two Cr-bonded carboxylate oxygen atoms of one complex. The Na–O distances lie between 2.363 (2) and 2.473 (2) Å, and the cis bond angles range from 80.01 (8) to 102.01 (7)°. The structure contains hydrogen bonds of the type N–H⋯O, W–H⋯S, and W–H⋯O, where W is a water oxygen atom.

Introduction

The interactions of sulfur-containing amino acids and their derivatives with transition metal ions have been a subject of great interest in recent years because of the potential use of these ligands in metal chelation therapy.[2a] Among cysteine derivatives, penicillamine (β,β′-dimethylcysteine) and N-acetylpenicillamine are clinically used for the treatment of metal poisoning.[2b–5] Nevertheless, in this field, the knowledge of the nature and the extent of the metal bonding to cysteine and its derivatives is of primary importance and this is best obtained from x-ray structural studies. Up to now, only a limited number of such crystallographic determinations is available. These include several mercury complexes of pen (penicillamine)[6–8] and cys (cysteine),[9] lead[10] and cadmium complexes of D-pen,[11] $Cu^{I}_8Cu^{II}_6(\text{D-pen})_{12}Cl$,[12] $Pd(SMC)Cl_2$ (SMC is S-methylcysteine),[13] $Co^{III}(SMC)_2^+$,[14] $Co^{III}(\text{L-his})(\text{D-pen})$,[15,16] $[Co_2^{III}(\text{L-his})(\text{D-pen})(\text{D-his})(\text{L-pen})]$,[15] $Cr^{III}(\text{L-his})(\text{D-pen})$,[15,16] $Co^{III}(\text{D-pen})(\text{L-pen})$,[17] and several complexes of Mo[18–21] with L-cys or its methyl or ethyl esters. Cysteine and its derivatives present three potential coordination sites for metal binding, these being S, N, and O. The structural studies have shown that in all cases the sulfur atom is coordinated to the metal and that one or two of the other sites are sometimes also involved. This contrasts with metal complexes of methionine, for which sulfur coordination to the metal ions has not been found in the complexes with Cd,[22] Zn,[23] and Cu,[24] although it does occur in complexes with Hg,[6] Pd,[25] and Pt.[26] Structural studies of metal complexes of cys and its derivatives also show that the metal–ligand bond distances vary widely. In some cases, one bond is much weaker than the others, but in other examples all bonds are apparently of approximately equal strength. To this last class belong the tridentate complexes formed between pen and Co(III) and Cr(III).

Crystal structure analyses of $Na[Cr(\text{L-cys})_2]\cdot 2H_2O$ have recently been carried out independently at Chapel Hill and